

Supporting Information for

Impacts of reservoir water level fluctuation on measuring seasonal seismic travel time changes in the Binchuan basin, Yunnan, China

Chunyu Liu¹; Hongfeng Yang^{2,1}, Baoshan Wang³, and Jun Yang⁴

¹Shenzhen research institute, The Chinese University of Hong Kong, Shenzhen, China

²Earth System Science Program, The Chinese University of Hong Kong, Hong Kong, China

³School of Earth and Space Science, University of Science and Technology of China, Hefei, China

⁴West Yunnan Earthquake Forecasting Experiment Site, China Earthquake Administration, Dali, Yunnan, China

Contents of this file

1. Introduction
2. Figure S1
3. Figure S2
4. Figure S3
5. Figure S4
6. Figure S5
7. Figure S6
8. Figure S7
9. Figure S8
10. Figure S9
11. Figure S10

Introduction

This supporting information provides additional figures used in the main article.

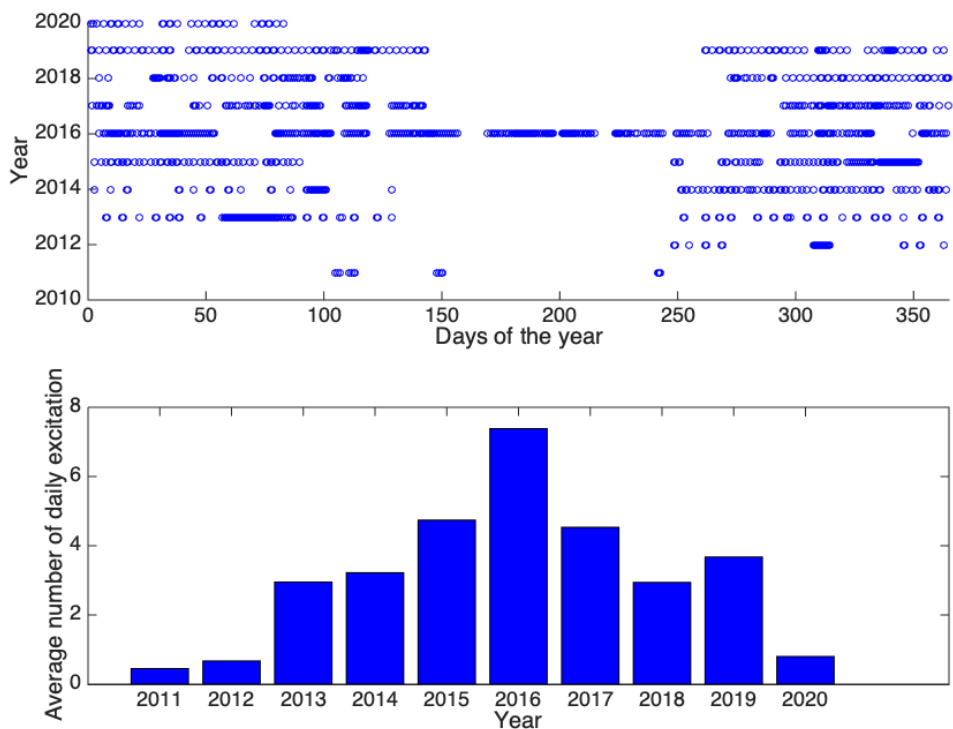


Figure S1. Airgun excitation time from 2011 to 2020 (Up) and the number of average daily excitation (Down).

From June to August, the water level in the reservoir is too low so it is not suitable for the airgun to operate.

Data is more complete in 2016 than other. The number of average daily excitation is 7 times/day in 2016.

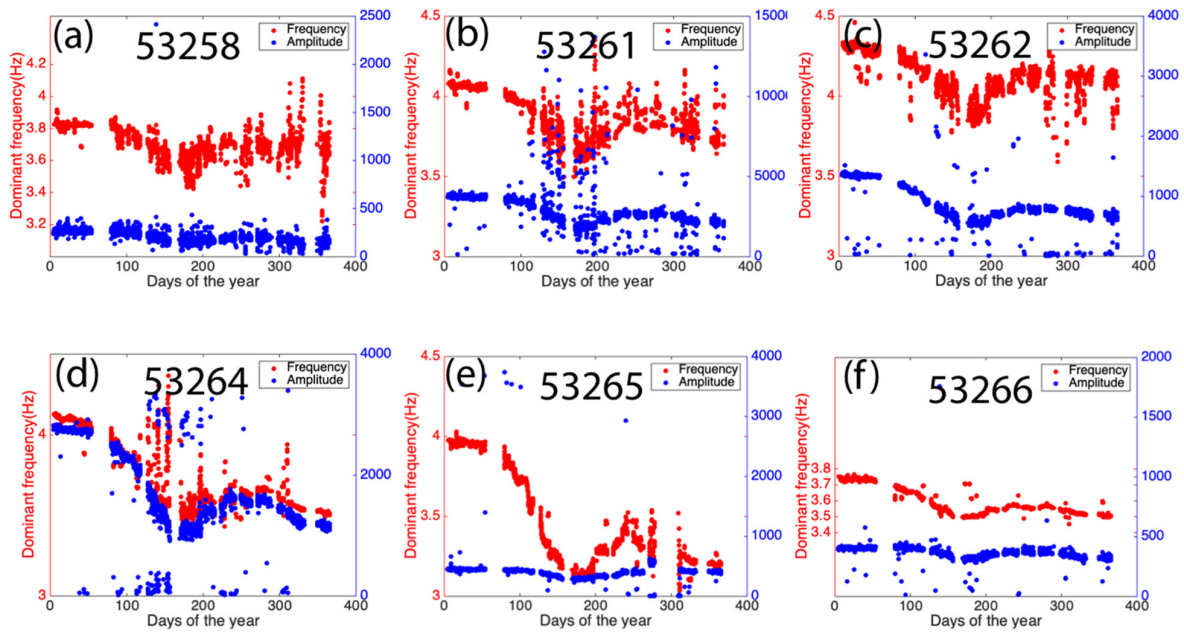


Figure S2. Seasonal change of the dominant frequency and signal amplitude.

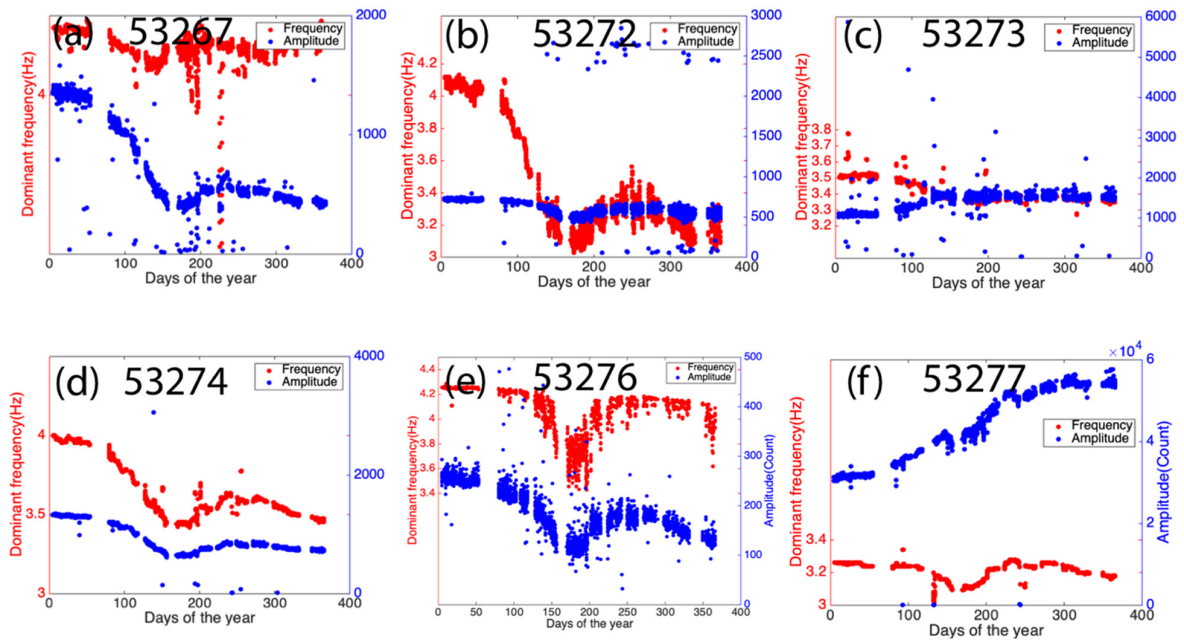


Figure S2. (Continued).

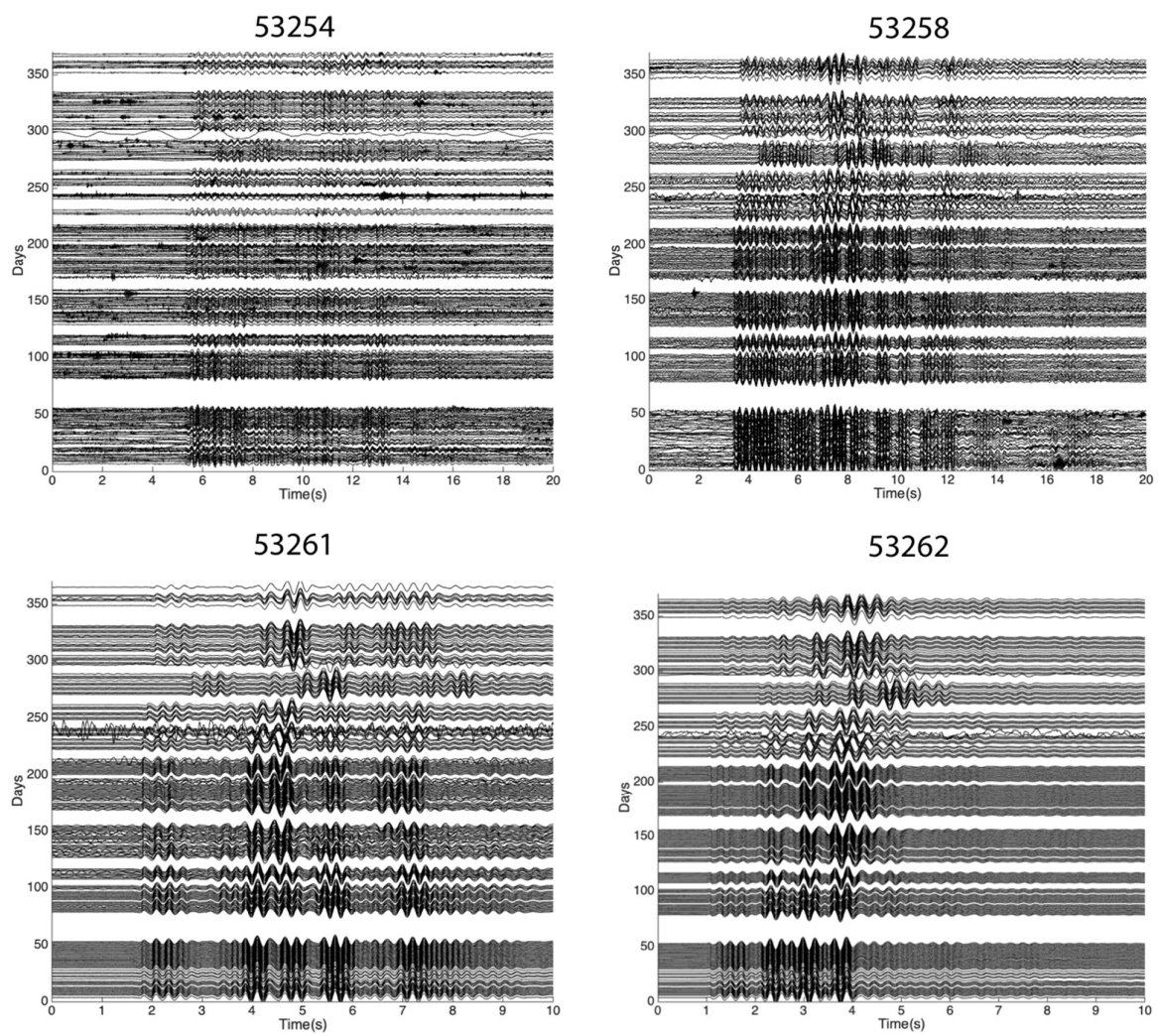


Figure S3. Different Airgun shots in 2016 at different stations. We observe strong clock drifts.

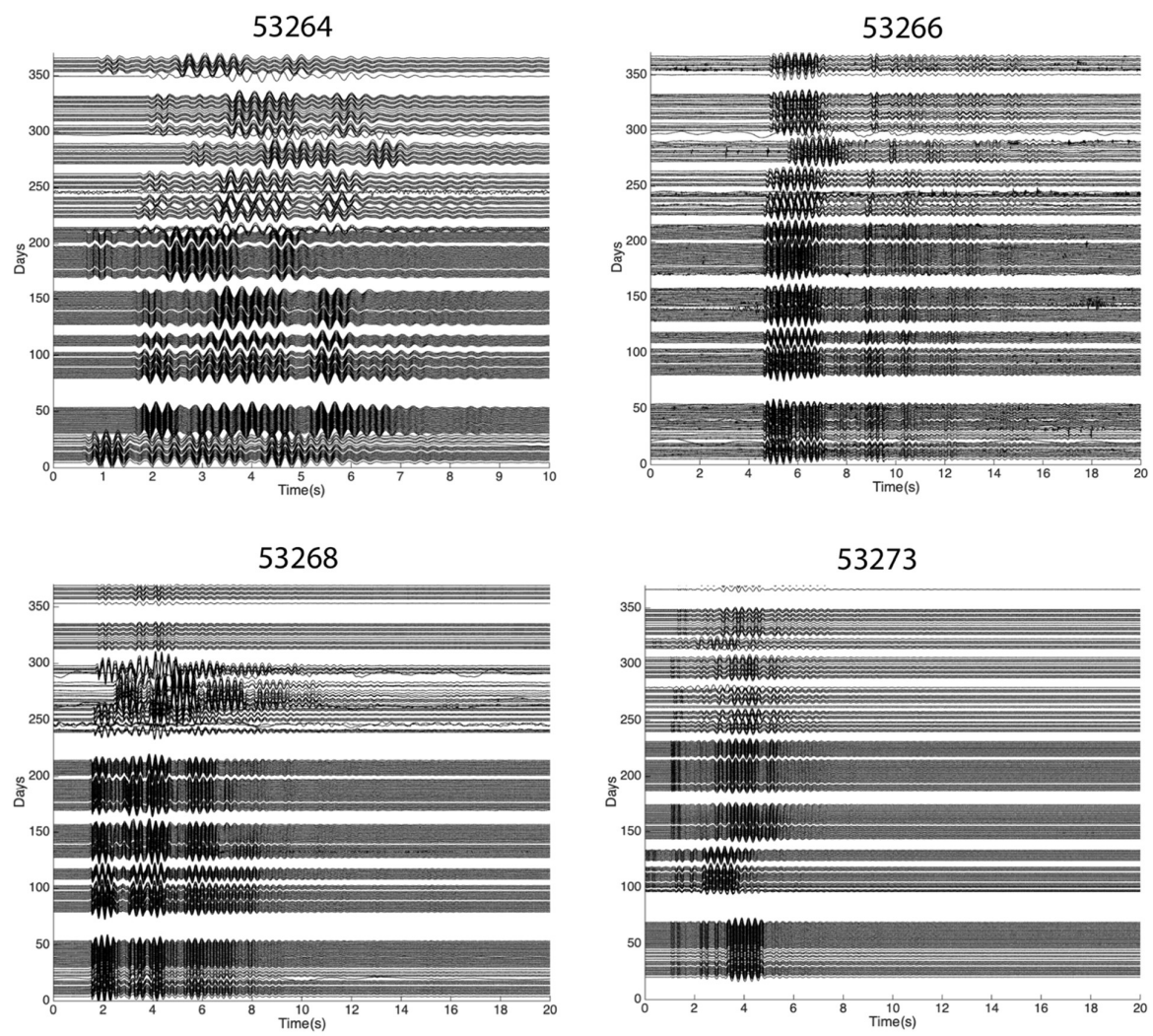


Figure S3. (Continued).

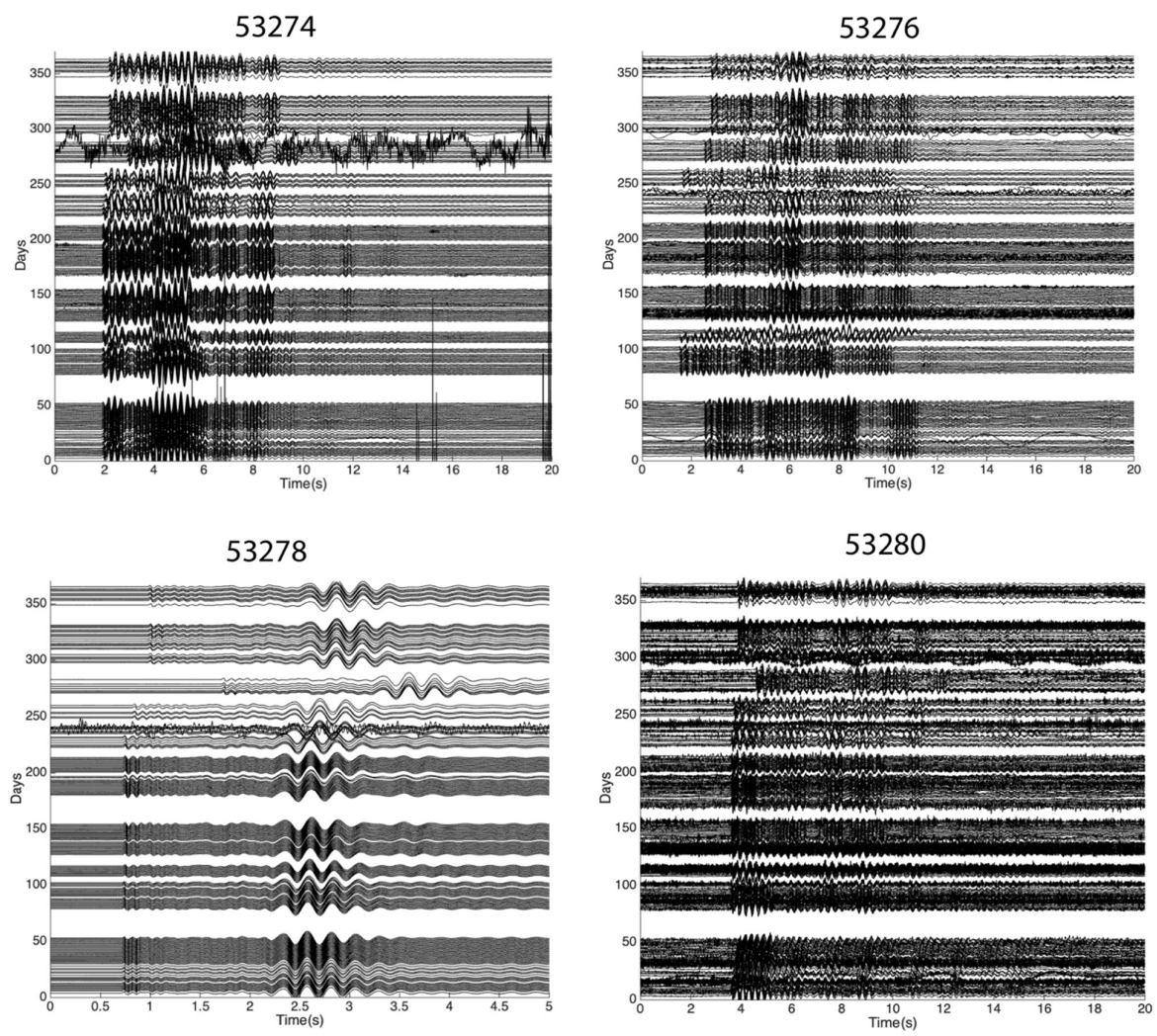


Figure S3. (Continued).

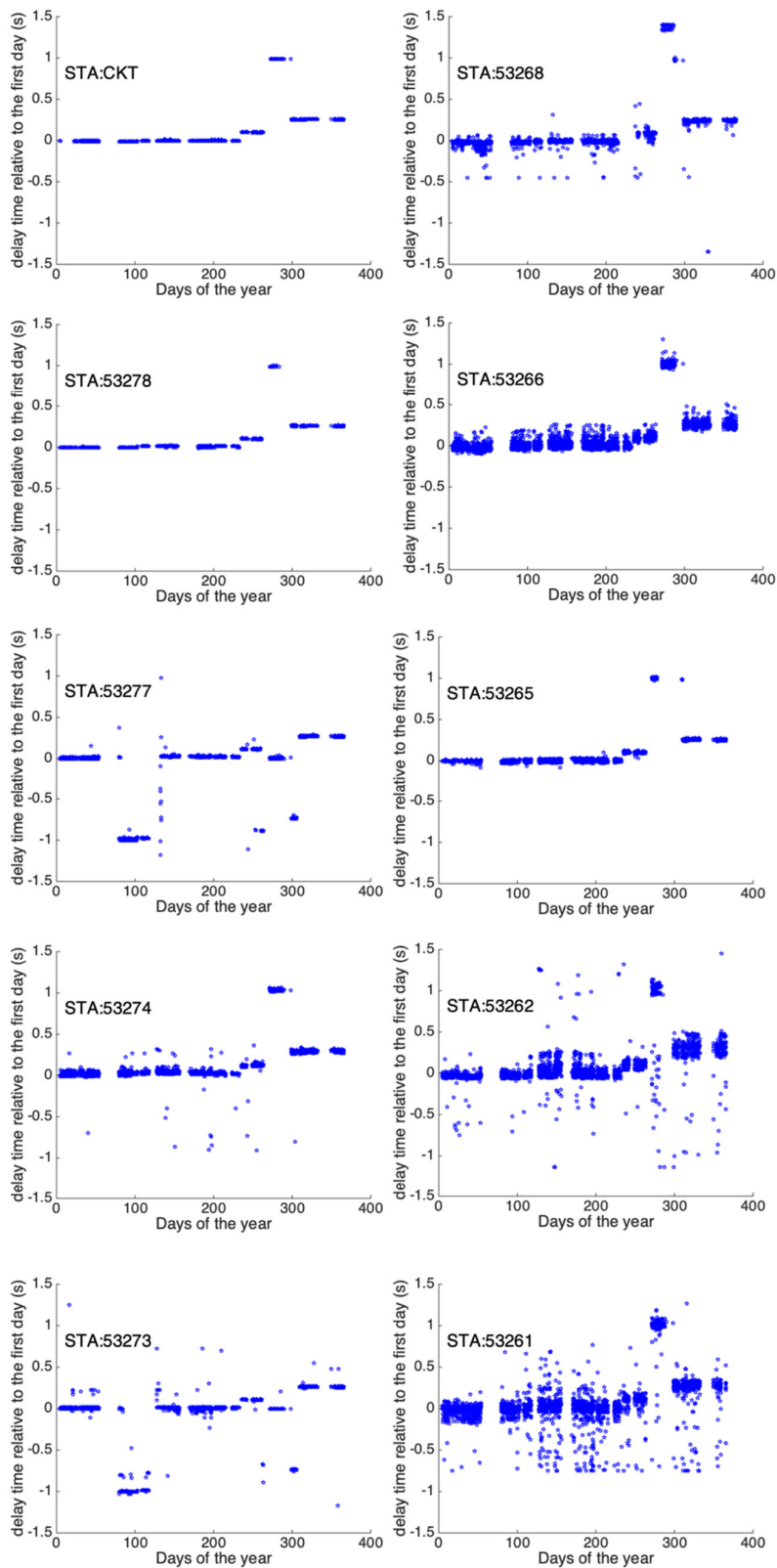


Figure S4. Delay time of P-wave arrivals relative to the time in the first day of 2016.

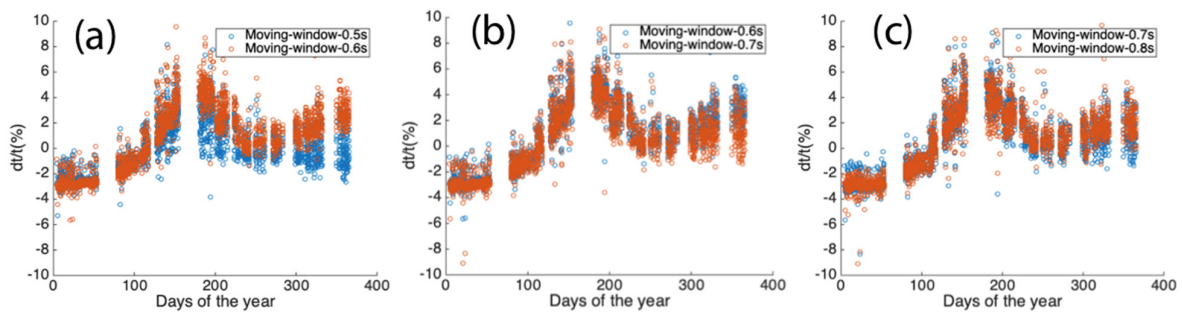


Figure S5. Seismic travel time change for station 53278 using different moving windows. We observe that the estimation of seismic travel time change is more stable when the length of the window is longer than 0.5s.

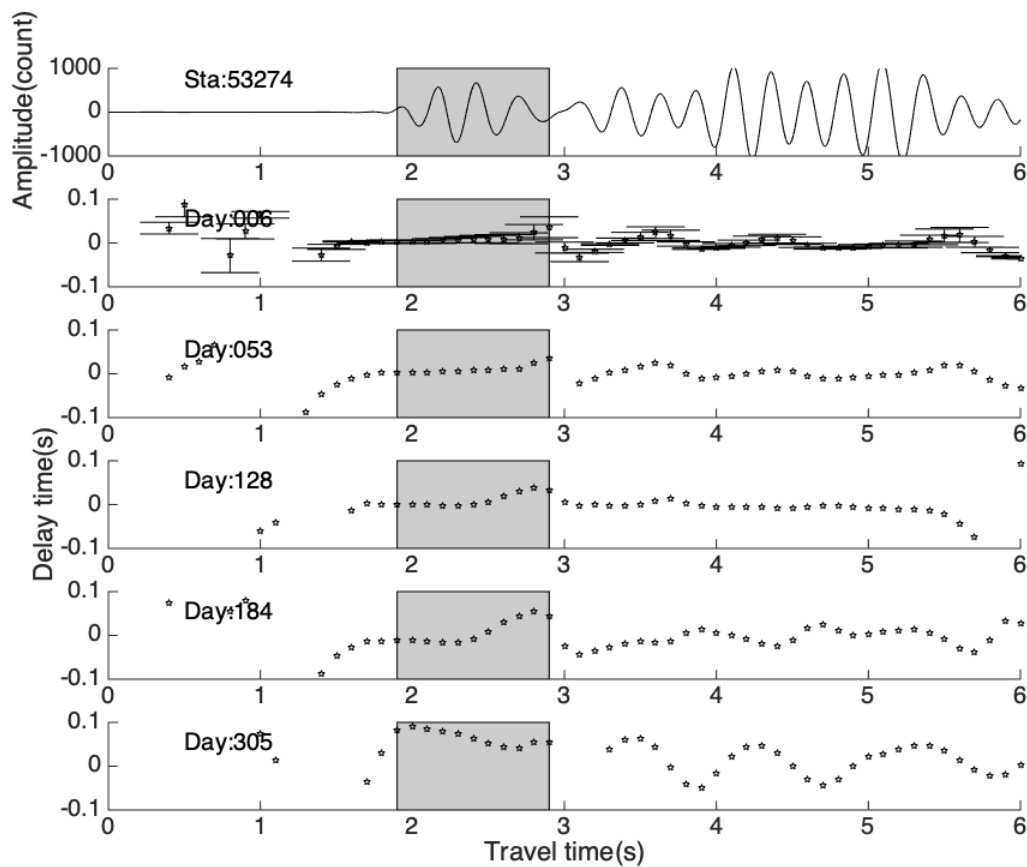


Figure S6. Determination of window for P-wave arrivals. We inspect the waveform to get a rough estimate of the begin and end time of P-wave arrivals. We then handpick the exact arrival time of P-wave based on the linearity of data points in the diagram of delay time verse travel time in different days.

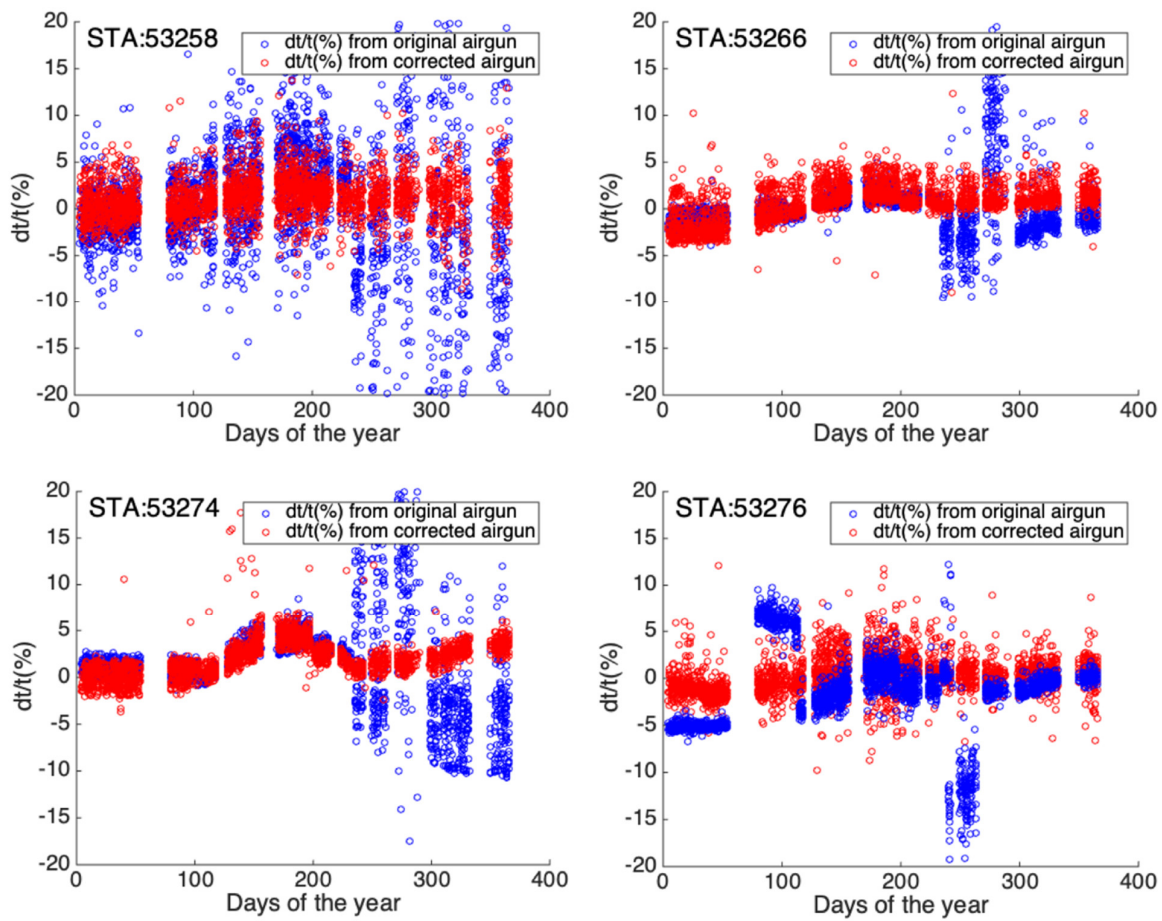


Figure S7. $\delta t/t$ measurements on P-wave arrivals at four stations with or without clock drift correction.

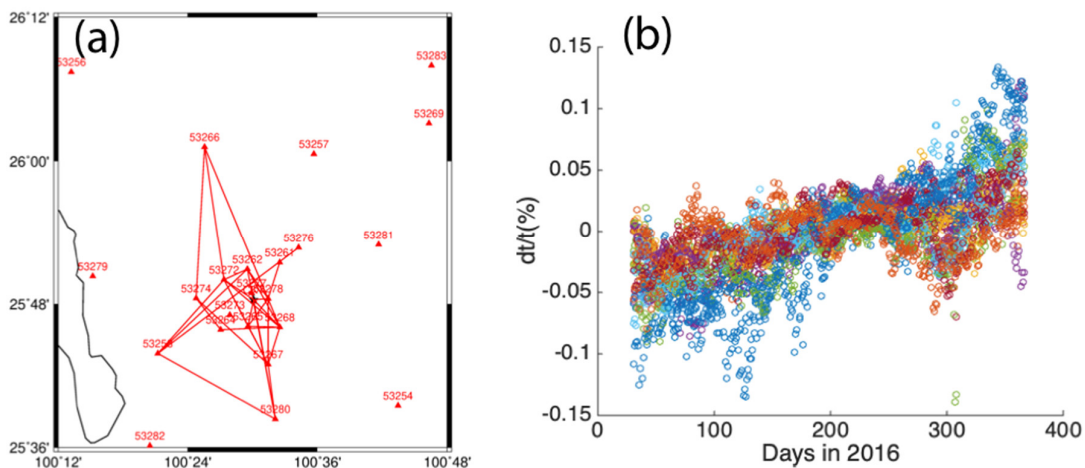


Figure S8. (a) Station pairs with similar seasonal changes of seismic travel time distribute in a broad region, at most 30 km from the reservoir. (b) 29 out of 91 station pairs show similar seismic travel time change $\delta t/t$.

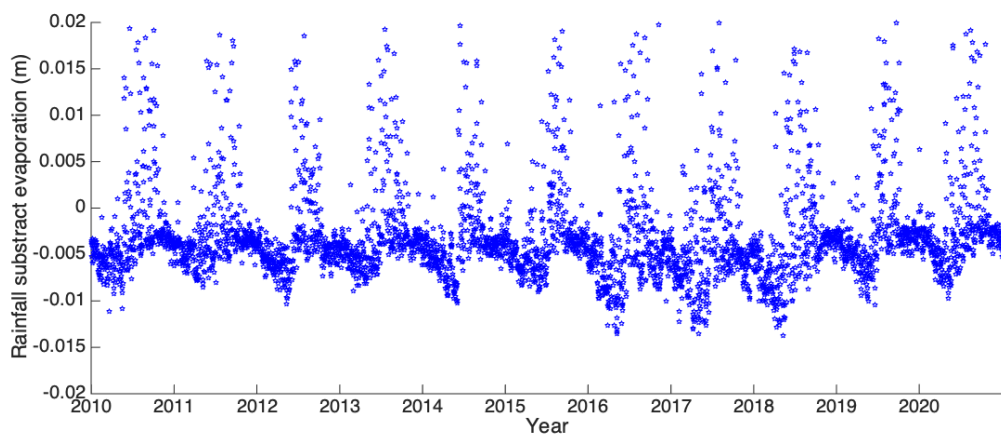


Figure S9. Precipitation subtracts evaporation.

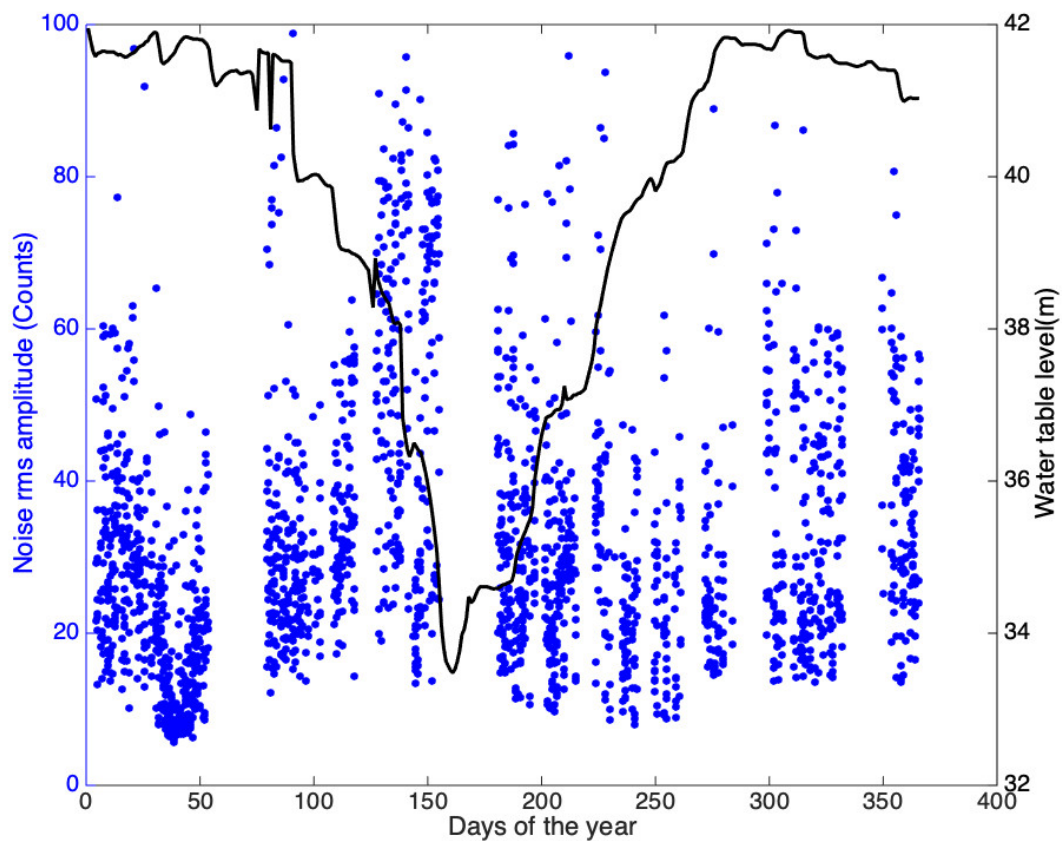


Figure S10. Ambient noise amplitude increases in the summer when the water level in the reservoir decreases. The increasing noise amplitude in the summer might be related to active anthropogenic activities.